Prenucleation at the Interface Between MgO and Liquid Magnesium: An *Ab Initio* Molecular Dynamics Study

C.M. FANG and Z. FAN

Magnesia (MgO) particles inevitably exist in liquid Mg and may be used as potential sites for heterogeneous nucleation to achieve effective grain refinement. Understanding of the atomic configurations on MgO surfaces and in the liquid Mg adjacent to the liquid Mg/MgO interfaces is therefore of both scientific and practical interests. We investigate the surface structures of MgO in liquid Mg and the atomic arrangements of liquid Mg adjacent to liquid/substrate interfaces, using an *ab initio* molecular dynamics (MD) simulation technique. We find that an atomically rough terminating Mg layer forms on the {1 1 1} terminated MgO substrate (octahedral MgO) in liquid Mg. The simulations also reveal that on the structurally flat {0 0 1} terminated MgO substrate (cubic MgO) a rough Mg layer forms due to the unique chemical interactions between the ions on the substrate and the liquid metals. The surface roughness together with the large lattice misfits with solid Mg makes both octahedral and cubic MgO substrates impotent for heterogeneous nucleation of α-Mg. The present results may shed new light on grain refinement of Mg-alloys.

https://doi.org/10.1007/s11661-019-05495-4

I. INTRODUCTION

GRAIN refinement is usually desirable during metal casting since it not only facilitates the casting processes, but also accomplishes a grain refined microstructure with reduced cast defects, which in turn enhances mechanical performance of as-cast components.[1–4] A well-established approach to grain refinement enhances heterogeneous nucleation by addition of grain refiners which contain potent solid particles as nucleation sites.[1,2] A typical example is the grain refinement of Al-free Mg-alloys by addition of Mg-Zr master alloys.[2,4–10] Zr is iso-structural to Mg with a small lattice misfit (0.67 pct), and therefore Zr particles should act as potent nucleation sites for α-Mg during solidification according to the epitaxial nucleation model.[11] Recently, a new concept of grain refinement was introduced based on the concept of explosive grain initiation, in which the most effective grain refinement can be achieved by the least potent particles if there exist no other more potent particles of significance in the melt.[12] This new approach to grain refinement can be best demonstrated by grain refinement of Mg-alloys by the native MgO particles.[13] Without addition of any grain refiner, high pressure die casting of commercial purity Mg resulted in an average grain size of 6 μm.[12] To understand better such experimental results and to obtain new insight into the heterogeneous nucleation process, it is essential to have detailed knowledge about the surface structures of MgO particles in contact with liquid Mg and the atomic arrangement in the liquid adjacent to the liquid Mg/MgO interfaces (denoted as L-Mg/MgO interfaces hereafter).

Magnesia (MgO) particles always exist in Mg melts due to the high affinity between O and Mg. MgO has a NaCl-type structure. It is a typical ionic crystal and belongs to the family of MX (M represents a metallic element, X an element of high electronegativity). The ionic MX crystals under ambient conditions have a stable {0 0 1} surface termination (denoted as MX{0 0 1} hereafter), which contains equal numbers of M^{n+} and X^{n-} ions and therefore are non-polar.[14] A cleavage along the MX[1 1 1] orientation produces two smooth surfaces: one with the M surface termination, the other with X surface termination, with both surfaces being polar. Such polar surfaces are unstable under ambient conditions, but can be stabilized by defects, *e.g.*, M or X domains.[15] However, the situation may become different when an ionic crystal is in a liquid metal environment. The free electrons of the liquid metal can eliminate the polar effect and stabilize the polar surfaces, such as in the case of MgO{1 1 1} in liquid Mg. MgO{1 1 1} surfaces have a two dimensional hexagonal lattice,

C.M. FANG and Z. FAN are with the BCAST, Brunel University London, Uxbridge, Middlesex UB8 3PH, United Kingdom. Contact e-mail: Zhongyun.Fan@brunel.ac.uk
Manuscript submitted 3 December, 2018.
Article published online December 9, 2019

the same as that of the close packed Mg{0 0 0 1} plane. However, there exists a large lattice misfit between MgO{1 1 1} and Mg{0 0 0 1} (8.2 pct),[12,16] rendering MgO particles impotent for heterogeneous nucleation of Mg.

There have been both experimental and modeling efforts to understand the nucleation of α-Mg on native MgO particles.[13,16–21] Native MgO particles in Mg melts have two distinctive morphologies: octahedron with {1 1 1} surface terminations (denoted as MgO{1 1 1}) and cubic with the {0 0 1} surface terminations (denoted as MgO{0 0 1}).[12,13,16–19] Experimental investigations by high-resolution transmission electron microscopy (HRTEM) have confirmed that there exist specific orientation relations (ORs) between the MgO substrates and the solid Mg. This suggests that fcc MgO can act as sites for heterogeneous nucleation of hcp α-Mg. First-principles approaches were used to explore mainly the wetting and adhesion for different crystal orientations between solid α-Mg and MgO.[20–22] In order to understand the structural effect on prenucleation at atomic level, Men and Fan[23,24] performed atomistic molecular dynamics (MD) simulations on the atomic ordering in a liquid metal adjacent to a smooth substrate of different lattice misfits. Their simulations showed that the structural effect is strong on the in-plane atomic ordering but weak on the atomic layering in the liquid adjacent to the substrate. A smooth substrate surface of a smaller misfit provides better structural templating for heterogeneous nucleation, in agreement with the epitaxial nucleation model.[11] Recently we investigated the chemical effect of potent substrates on prenucleation and found that a chemically affinitive substrate promotes prenucleation in the liquid at the liquid/substrate interface, whereas a chemically repulsive substrate impedes it.[25] In addition, Jiang *et al.*[26] modeled the effect of substrate surface roughness on prenucleation using a classic atomistic MD technique. Their modeling revealed that atomic level surface roughness impedes significantly prenucleation.[26] In light of such findings, it would be interesting to investigate the effect of interaction between MgO and liquid Mg on the prenucleation at the L-Mg/MgO interface.

In this paper, we investigate systematically the prenucleation phenomenon in L-Mg/MgO{1 1 1} and L-Mg/MgO{0 0 1} systems using a parameter-free *ab initio* molecular dynamics (*AI*MD) technique. The simulation results suggest that both MgO{1 1 1} and MgO{0 0 1} are impotent for heterogeneous nucleation of α-Mg. Such information is not only helpful to understand heterogeneous nucleation theory in general, but also facilitates the development of effective approaches to grain refinement of Mg-alloys.

II. SIMULATION METHODS

A. *Setting Up Supercells for Simulations*

Periodic boundary conditions were employed in the structural optimizations and the *AI*MD simulations. A hexagonal supercell was built based on the relation of $a \approx 3.615 a_o$, where a_o is the lattice parameter of the fcc MgO.[27] The substrate is composed of four O layers and three Mg layers (O-terminated) or four O layers and five Mg layers (Mg-terminated). In this way the hexagonal supercell has $a = 14.90$ Å, and $c = 64.62$ Å, and contains 425 Mg and 100 O for the L-Mg/MgO{1 1 1} systems, with consideration of the thermal expansion of both MgO and Mg at 1000 K.[27,28] The melting temperature of Mg is 650 °C or 923 K at ambient pressure. Similarly, a tetragonal supercell with $a = 16.85$ Å and $c = 35.05$ Å was built for the L-Mg/MgO{0 0 1} system. This supercell contains 320 atoms in liquid Mg and 192 atoms in MgO substrate. We employed these large supercells in order to avoid risk of artificial crystallization of the liquid Mg, and to achieve a good balance between the simulations reliability and the computational capability.

B. *Quantifying Atomic Ordering in the Melt Adjacent to a Substrate*

To quantitatively describe the atomic ordering of the liquid Mg adjacent to the substrates, two different parameters were used.[23,29] One is the atomic density profile, $\rho(z)$:

$$\rho(z) = \langle N_z(t) \rangle / (L_x L_y \Delta z), \quad [1]$$

where L_x and L_y are the x and y dimensions of the cell, respectively, and z the dimension perpendicular to the interface, Δz the bin width, and $N_z(t)$ the number of particles between $z - (\Delta z/2)$ and $z + (\Delta z/2)$ at time t. $\langle N_z(t) \rangle$ indicates a time-averaged number of particles. The atomic density profile, $\rho(z)$, describes atomic ordering along the z-direction.

Another one is the in-plane order parameter, $S(z)$, which is used to quantify the degree of atomic ordering in each layer and is defined as[23,29]:

$$S(z) = [\sum \exp(i \boldsymbol{Q} \cdot r_j)]^2 / N_z^2, \quad [2]$$

where the summation is over all atoms within a given bin of width Δz, $\boldsymbol{Q}$ is the reciprocal lattice vector, and $\boldsymbol{r}_j$ is the Cartesian coordinates of the jth atom in space, N_z the number of atoms in the bin. $S(z)$ quantifies the atomic ordering in a plane parallel to the interface.

C. *Simulation Technique and Settings*

In this study, we employed a pseudo-potential plane-wave approach within the first-principles density-functional theory (DFT) code Vienna *ab initio* Simulation Package (VASP).[30,31] The VASP code uses the projector augmented-wave (PAW) method.[32,33] The exchange and correlation terms are described using the generalized gradient approximation (GGA-PBE).[34] The atomic electronic configurations in pseudo-potentials are Mg ([Ne] $3s^2 3p^0$) and O ([He] $2s^2 2p^4$). The cut-off energies for the wave functions and for the augmentation functions for structural optimizations were 400.0 and 600.0 eV, respectively. The electronic

wave functions were sampled on dense grids, *e.g.*, a 24 × 24 × 24 *k*-mesh (365 ***k***-points) in the irreducible Brillouin zone (BZ) of the conventional face-centered cubic (fcc) cell of MgO using the Monkhorst–Pack approach.[35] The present method allows variable fractional occupation numbers. Therefore, it works well for metallic systems. This code has been successfully applied to simulate metallic/insulating transition,[30,31] as well as solid/liquid interface systems.[25] The *ab initio* MD simulation is based on the finite-temperature density-functional theory of the one-electron states. It is also based on the exact energy minimization and calculation of the exact Hellmann–Feynman forces after each MD step using the preconditioned conjugate techniques, and the Nosé dynamics for generating a canonical NVT ensemble.[30] For the *AI*MD simulations of the large supercells, we employed a cut-off energy of 320 eV for the L-Mg/MgO systems, and only the Γ-point in the BZs to balance the demand of computations for obtaining reliable results and capability of the computer cluster. Test simulations using different cut-off energies ranging from 200.0 to 400.0 eV have shown that the present settings are reasonable.

The liquid Mg of the systems was generated by equilibrating for 3000 steps (1.5 fs per step) at 3000 K. The equilibrated liquid Mg at high temperature was then cooled to the designed temperatures. The obtained liquid Mg and the substrates were used to build the simulation systems for equilibrating at the designed temperature for about 6000 to 8000 steps (about 10 ps). It is well known that for complex liquid/solid systems, a meaningful statistical analysis cannot be drawn from a single model, and conclusions based on limited configuration-sampling might be misleading.[25,30,36,37] In the present study, we used several different starting structures, and employed the time-averaged method to sample the system with over a period of time up to 4.5 ps (3000 steps) to obtain meaningful results. All substrate and liquid atoms were fully relaxed during the simulations.

III. RESULTS

The first-principles DFT structural optimizations were conducted to calculate lattice parameters of both hcp α-Mg and fcc MgO. The calculated lattice parameters for α-Mg are $a = 3.192$ Å and $c = 5.185$ Å, which are very close to the experimental values of $a = 3.2094$ Å, $c = 5.2108$ Å in the literature.[28] The calculated lattice parameter for the MgO is $a = 4.246$ Å, which is again very close to the experimental value of $a = 4.212$ Å.[27] Both calculations reproduced the experimental values well within 1 pct of error, confirming the validity of the current simulation approaches.

A. *Surface Structures of the MgO Substrates in Liquid Mg*

The MgO{1 1 1} surface has two potential atomic configurations; one is O-terminated (denoted as MgO{1 1 1}$_{O}$) and the other one is Mg-terminated (denoted as MgO{1 1 1}$_{Mg}$). In this work we have simulated atomic arrangements in liquid Mg adjacent to both MgO{1 1 1}$_{O}$ and MgO{1 1 1}$_{Mg}$ substrates. Figure 1 shows the evolutions of atomic arrangements at the L-Mg/MgO{1 1 1} interfaces during the *AI*MD simulations at 1000 K.

The Mg atoms in the liquid adjacent to the MgO{1 1 1}$_{O}$ substrate approach quickly the surface of MgO{1 1 1}$_{O}$ substrate (Figures 1(a) through (c)). A stable Mg layer forms on the MgO{1 1 1}$_{O}$ substrate and became the new terminating layer of the substrate. Similarly, for the L-Mg/MgO{1 1 1}$_{Mg}$ system, during the *AI*MD simulations the liquid Mg atoms move to the substrate to reach thermal equilibrium (Figures 1(d) through (f)). It is confirmed that after about 1500 steps (2.25 ps), the systems reached thermal equilibrium. The resultant equilibrium atomic configurations at terminating surfaces of both substrates are presented in Figure 2. Figure 2(a) shows that some of the Mg atoms at the MgO{1 1 1}$_{Mg}$ surface has moved away and became part of the liquid, leaving a substantial amount of vacancies (marked by the crosses) on the surface layer. The newly formed terminating layer on the MgO{1 1 1}$_{O}$ substrate (Figure 2(b)) also contains vacancies (marked by the crosses). A close examination of Figures 2(a) and (b) revealed that there is no notable difference in atomic configurations at the terminating substrate surfaces with two different starting structures (Figures 2(a) and (b)). This suggests that the interaction between the MgO{1 1 1} substrate and the liquid Mg leads to the formation a new terminating surface layer which has a hexagonal atomic arrangement of Mg atoms and contains certain amount of vacancies, regardless atomic configuration of the starting substrate surface. Therefore, it can be concluded that the MgO{1 1 1} substrate in contact with liquid Mg is atomically rough due to the existence of vacancies.

B. *Effects of the Substrate Surfaces on Prenucleation*

Figure 3 shows snapshots of the thermally equilibrated L-Mg/MgO{1 1 1} (Figure 3(a)) and L-Mg/MgO{0 0 1} (Figure 3(b)) interfaces at 1000 K. Figure 3 provides us with a direct impression about the atomic ordering in the liquid Mg adjacent to the substrates. The liquid Mg atoms in both the L-Mg/MgO{1 1 1} and the L-MgO{0 0 1} systems display rather weak layering. In both cases, there is only a few identifiable atomic layers for the liquid Mg near the substrate. These Mg atoms in such layers show significant mobility and exhibit dominantly liquid-like behavior. In addition, we noticed that there is a distinct separation between the liquid Mg atoms and the flat MgO{0 0 1}.

The density profile of liquid Mg atoms perpendicular to a substrate surface, $\rho(z)$, provides a quantitative description of the atomic layering phenomenon.[11,23–25,29] We analyzed the density profiles based on the time-averaged atomic configurations of the simulated systems for over 3 to 6 ps using Eq. [1]. The results are shown in Figure 4 for the density profiles $\rho(z)$ and in Figure 5 for the peak density profiles ρ_{peak}. The density profiles confirmed our first impressions about the layering phenomenon in Figure 3. Only 4 Mg layers

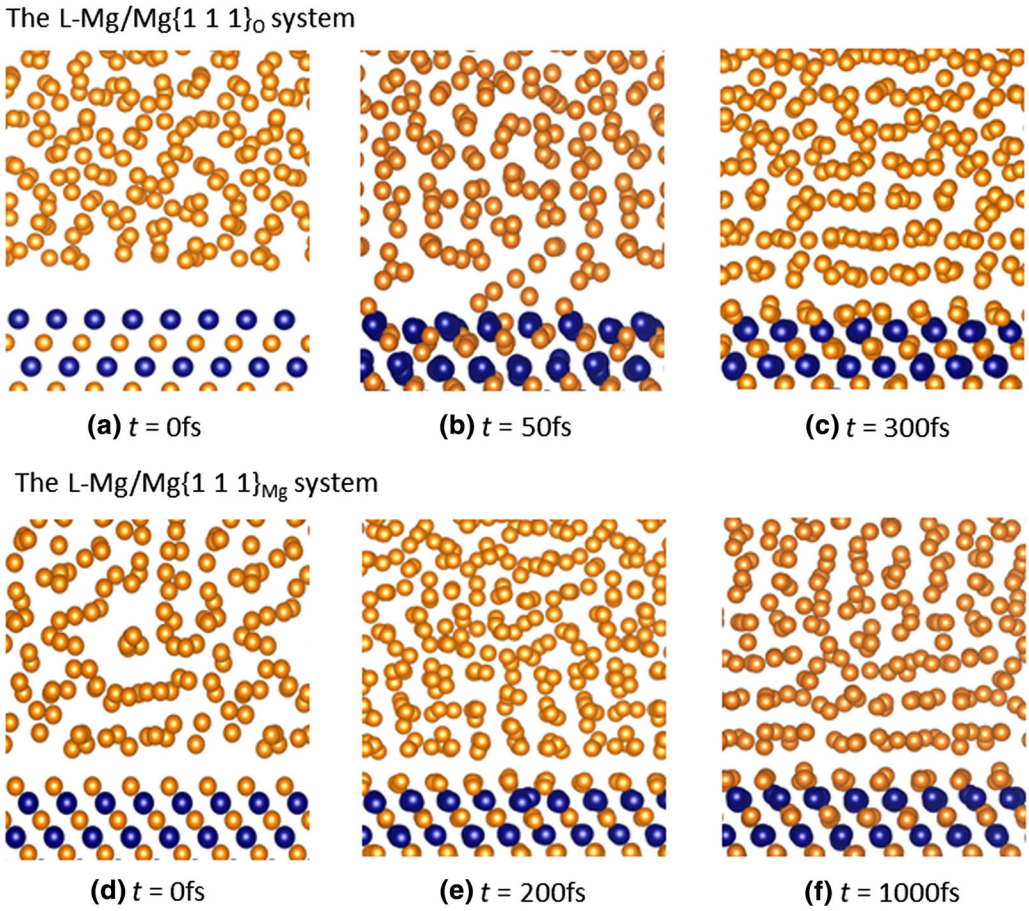

Fig. 1—Snapshots during *ab initio* molecular dynamics simulations at 1000 K showing the evolution of atomic configurations in the L-Mg/MgO{1 1 1} systems from different starting configurations. (*a*) through (*c*) the L-Mg/MgO{1 1 1}$_O$ system; and (*d*) through (*f*) the L-Mg/MgO{1 1 1}$_{Mg}$ system. The golden spheres represent Mg atoms, and the dark blue spheres represent O atoms (Color figure online).

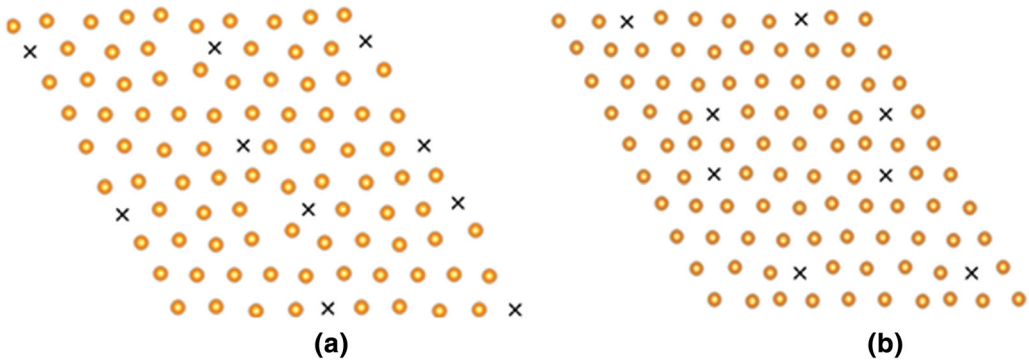

Fig. 2—Snapshots of atomic configurations (about 1ps) in the newly formed terminating Mg layer on the MgO{1 1 1} surfaces simulated at 1000 K from different starting surface configurations, (*a*) the L-Mg/MgO{1 1 1}$_O$ system; and (*b*) the L-Mg/MgO{1 1 1}$_{Mg}$ system. The golden spheres represent Mg atoms and the crosses for vacancies (Color figure online).

can be recognized in the L-Mg/MgO{1 1 1} system (Figure 4(b)) and 3 Mg layers in the L-Mg/MgO{0 0 1} system (Figure 4(a)). In both cases, the peak heights of liquid Mg layers are rather low as compared with those of the substrates and decrease with increasing distance from the interface (Figure 5).

The previous atomic molecular dynamics simulations revealed that there are generally six layers in liquid metal adjacent to a smooth metallic substrate.[23–25] There are only three atomic layers of liquid Al. The lattice misfit between MgO{1 1 1} and Mg{0 0 0 1} is 8.2 pct.[12,16] However, as shown in the literature, lattice misfit has

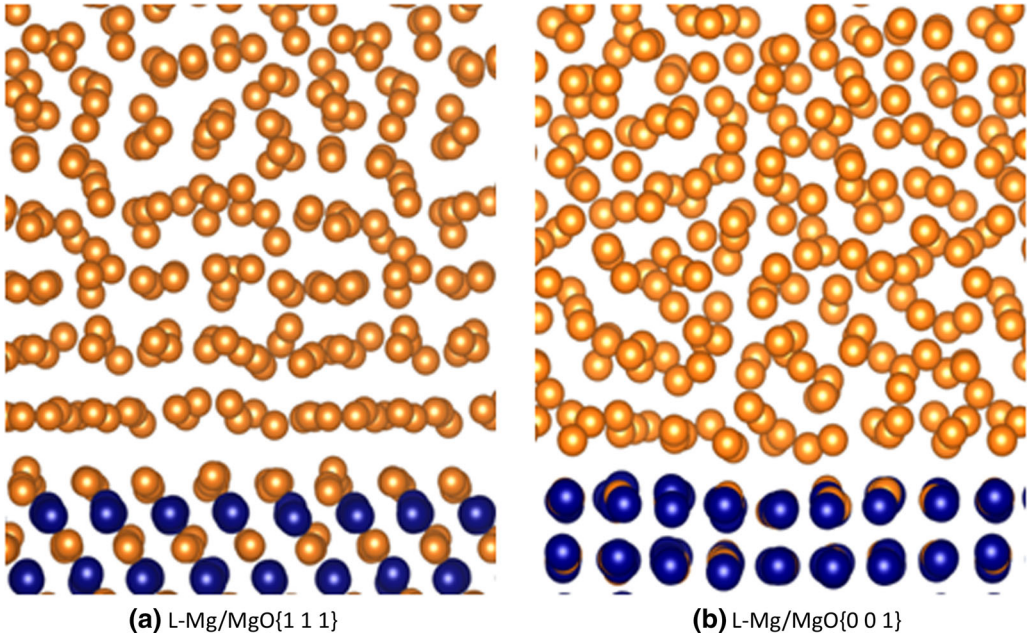

Fig. 3—Snapshots for (*a*) the L-Mg/MgO{1 1 1} and (*b*) the L-Mg/MgO{0 0 1} systems at thermodynamically equilibrated state at 1000 K. The golden spheres represent Mg atoms, and the dark blue spheres represent O atoms (Color figure online).

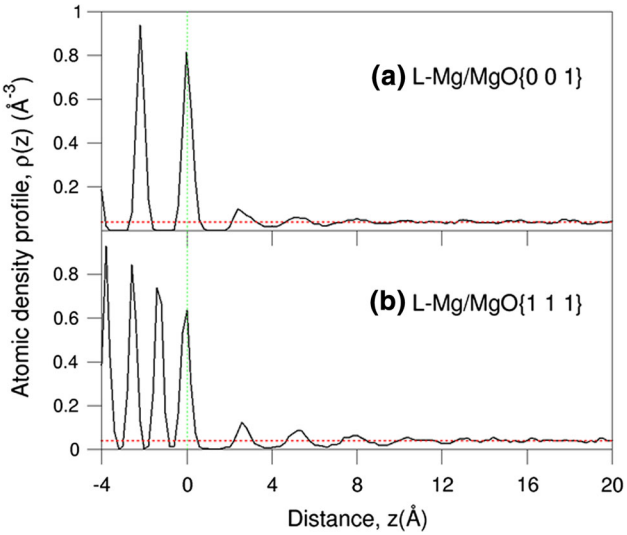

Fig. 4—Atomic density profiles, $\rho(z)$ for (*a*) the L-Mg/MgO{1 1 1} system; and (*b*) the L-Mg/MgO{0 0 1} system at thermodynamically equilibrated state at 1000 K. $z = 0$ marks the position of terminating surface of the substrate.

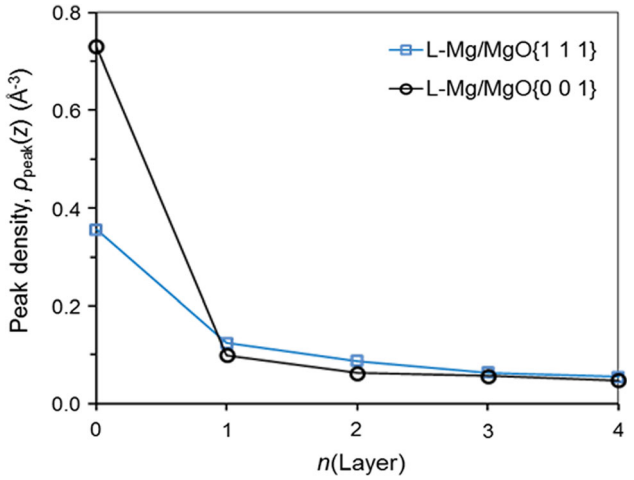

Fig. 5—Peak density, $\rho_{peak}(z)$ for the liquid layers in the L-Mg/MgO{1 1 1} and the L-Mg/MgO{0 0 1} systems at thermodynamically equilibrated state at 1000 K (Color figure online).

little influence on the layering of the liquid atoms adjacent to the substrate.[23,24] Therefore, we can conclude that the weakened layering in the L-Mg/MgO{1 1 1} system originates from the atomically rough substrate surface,[26] since the atomically rough surface hinders the templating of substrate for liquid Mg to nucleate, according to the epitaxial nucleation/growth model.[11]

Figure 4 also provides information about the interlayer spacing between the substrate surface layer and the 1st liquid Mg layer. The interlayer spacing between the 1st Mg peak and the peak of the terminating Mg surface of the L-Mg/MgO{1 1 1} system is about 2.60 Å, which is close to the interlayer spacing along the Mg[0 0 0 1] orientation (2.61 Å). This indicates that the chemical interaction between the MgO{1 1 1} substrate and the liquid Mg is neutral according to our previous work.[25] This will be discussed in the next section.

At the L-Mg/MgO{0 0 1} interface, the structurally flat MgO{0 0 1} surface does not promote the atomic layering in the liquid Mg. There are only three recognizable Mg peaks with low peak heights (Figure 4(a)). This is somewhat unexpected. Furthermore, a close look at the first liquid Mg peak of the L-Mg/MgO{0 0 1} system reveals that this Mg peak is asymmetrical.

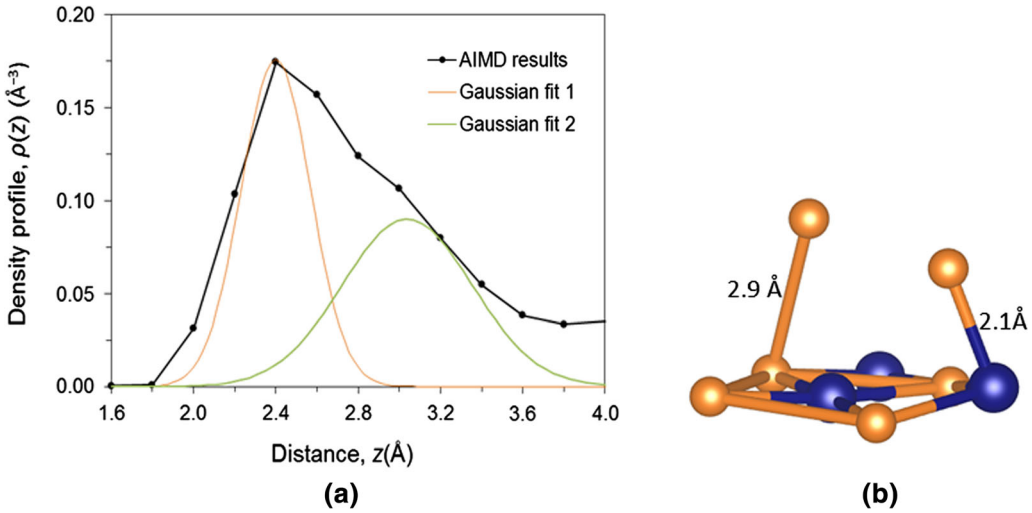

Fig. 6—(*a*) The density profile of the first liquid Mg layer in the L-Mg/MO{0 0 1} system and its decomposed Gaussian peaks; and (*b*) the chemical bonding of liquid Mg atoms to the adjacent oxygen and magnesium ions in the MgO{0 0 1} substrate. The golden spheres represent Mg atoms, and the dark blue spheres represent O atoms. The numbers in (b) mark the bond lengths (Color figure online).

The 1st Mg peak adjacent to the MgO{0 0 1} substrate surface is enlarged and analyzed, and the results are presented in Figure 6. Apparently, this broadened and asymmetrical Mg peak contains a peak and a shoulder. Accordingly, we deconvolute it into two peaks: a peak at the position of 2.4 Å and a shoulder centered at 3.2 Å with respect to the MgO terminating layer (Figure 6(a)). Our analysis showed that the high peak at 2.4 Å is composed mainly of Mg atoms close to the O ions of the MgO{0 0 1} substrate surface, whereas the shoulder at 3.2 Å consists of Mg atoms close to the Mg ions of the substrate surface (Figure 6b). It is noticed that the bond length between the Mg ion at the substrate surface and the Mg atom in the liquid is 2.9 Å, being 0.8 Å longer than that between the oxygen ion and the Mg atom in the liquid (Figure 6(b)). This corresponds well to the layer spacing difference between the peak and the shoulder (0.8 Å) in Figure 6(a). This indicates that the chemistry of the MgO{0 0 1} substrate surface causes the separation of Mg atoms in the 1st liquid Mg layer. Consequently, the 1st Mg layer is atomically rough, which strongly reduces its capability to template atomic ordering in the subsequent layers.

As suggested by the epitaxial nucleation model, heterogeneous nucleation occurs *via* a layer by layer growth mechanism.[11] Therefore, the atomic ordering in an atomic layer at the liquid/substrate interface is vital to understand the nucleation potency of a substrate. Figure 7 displays the atomic arrangements of the terminating substrate layer and the first two liquid Mg layers adjacent to the substrates. Figure 8 shows the quantified in-plane order parameters of the terminating substrate layers and the liquid Mg layers from atomic configurations integrated over 3 to 6ps, according to Eq. [2].

We first address the in-plane order parameters of the terminating layers of the substrates. As shown in Figure 7, the terminating layer of the structurally flat MgO{0 0 1} substrate shows high degree of in-plane ordering, whereas there are vacancies in the terminating layer of MgO{1 1 1} substrate. In spite of these difference, the in-plane ordering parameter of the terminating Mg layer in L-Mg/MgO{1 1 1} system is 0.59, which is even slightly higher than that of the structurally flat MgO{0 0 1} surface ($S(z) = 0.57$) (Figure 8).

Figure 7 also shows highly delocalized characteristics of the Mg atoms even in the first Mg layer on both MgO{1 1 1} and MgO{0 0 1} substrates. This indicates that these Mg atoms exhibit mainly liquid-like behavior in the first layer. Correspondingly, the values of the in-plane order parameter, $S(z)$ which was defined in Eq. [2] are small, being 0.01 for the 1st Mg layer on the MgO{1 1 1} substrate, and 0.08 for the first Mg layer on the MgO{0 0 1} substrate (Figure 8). Consequently, $S(z)$ is effectively zero for the subsequently Mg layers in both cases.

To sum up, *AI*MD simulations showed that both atomically rough MgO{1 1 1} substrate and the structurally flat MgO{0 0 1} substrate induce only weak atomic layering and little in-plane ordering in the liquid Mg adjacent to the L-Mg/MgO interface. This suggests that those MgO substrates have poor capability to template atomic ordering in the liquid Mg and are therefore impotent for heterogeneous nucleation of solid Mg during solidification.

C. *Chemical Interaction Between Substrates and Liquid Mg*

In order to obtain further insight into the atomic ordering in the liquid Mg adjacent to the substrate surface, we performed accurate electronic structure calculation and obtained electron density distributions for selected atomic configurations at the L-Mg/MgO interfaces. The iso-surfaces of electron density distributions ($\rho_0(r) = 0.017$ e/Å^3) of the investigated interfaces are presented in Figure 9. As shown in Figure 9, the

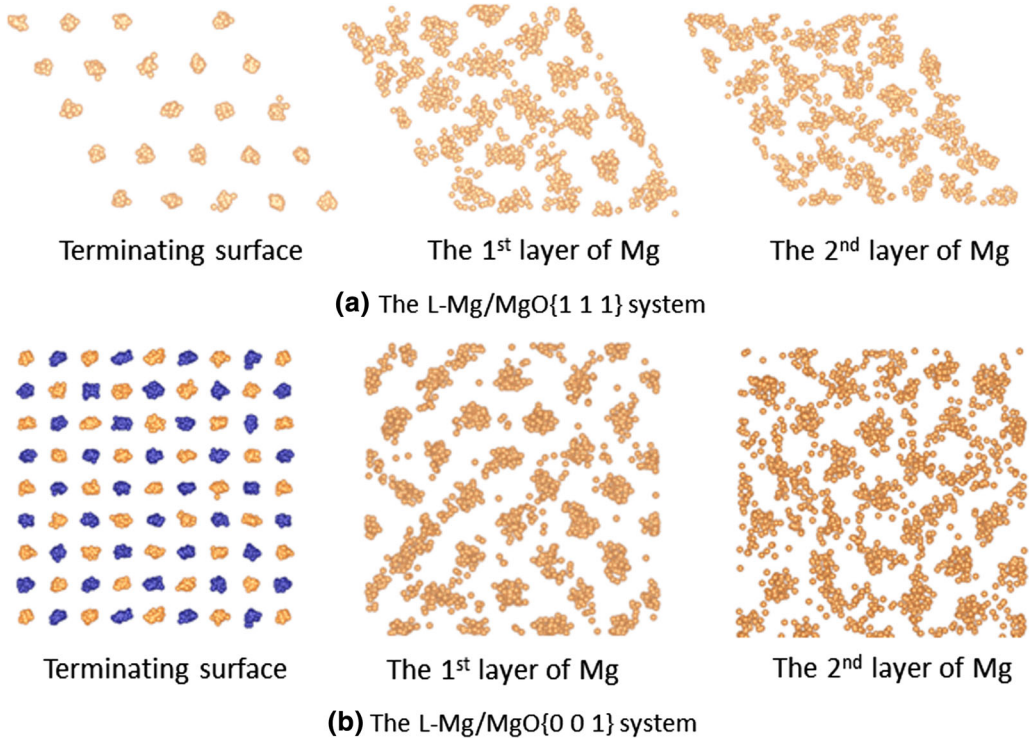

Fig. 7—Time-averaged atomic positions in the terminating surface layer and the first two liquid layers (*a*) for the L-Mg/MgO{1 1 1} system; and (*b*) for the L-Mg/MgO{0 0 1} system. The golden spheres represent Mg atoms, and the dark blue spheres represent O atoms (Color figure online).

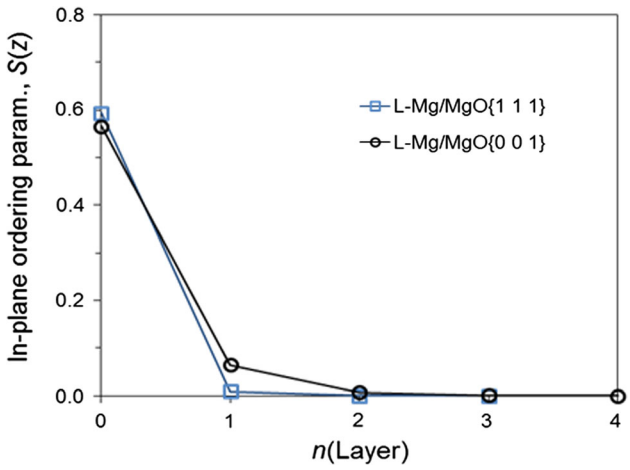

Fig. 8—In-plane order parameter, $S(z)$ of the liquid Mg atoms as a function of the atomic layers away from the L-Mg/MgO interfaces. The n(layer) = 0 represents the substrate surface (Color figure online).

electron density distributions of the MgO substrates show dominantly spherical-shaped electron clouds in the substrate regions. These spherical clouds belong to the oxygen ions. Meanwhile, there is little electron around the Mg ions/atoms in the MgO substrates. These results correspond well with the ionic nature of MgO. In addition, the liquid Mg regions are also composed of Mg ions and electron clouds, being consistent with the free electron nature of condensed Mg.

Charge transfer provides further information about the interfacial chemistry.[25,38] Bader provided a unique way to divide the boundaries of an ion/atom in a solid *via* the zero flux surfaces of the electron density distributions of a solid.[38] This model was implanted in the code VASP.[39] Figure 10 shows the net charges at the atomic sites for the L-Mg/MgO systems. As shown in Figure 10, all O ions in MgO substrates have the same net charge (− 1.3 e) and Mg ions in the substrates are positively charged with a loss of 1.3 e/Mg. This agrees with the large electronegativity difference between Mg (1.31 in Pauling scale) and O (3.44). Meanwhile, this charge transfer (1.3 e) is smaller than the pure ionic model (2.0 e), suggesting that although MgO is an ionic compound, it exhibits some covalent nature.

Figure 10 shows that the terminating Mg ions at the MgO{1 1 1} substrate surface are less charged (+ 0.6 e/Mg on average) as compared with those in the bulk substrate (+ 1.3 e/Mg). The Mg atoms in the first liquid layer on the MgO{1 1 1} substrate are electronically neutral. Therefore, the interaction between the substrate Mg surface and liquid Mg is dominated by metallic nature. This is consistent with the fact that the interlayer spacing between the terminating Mg layer and the 1st liquid Mg layer is 2.60 Å, close to that between Mg layers (2.61 Å) (Figure 4(b)).

Interestingly, liquid Mg atoms adjacent to the structurally flat MgO{0 0 1} substrate lose some electrons (Figure 10(b)). This means that charge transfer occurs from the liquid Mg to the substrate. This result justifies the interpretation of the splitting of the liquid Mg

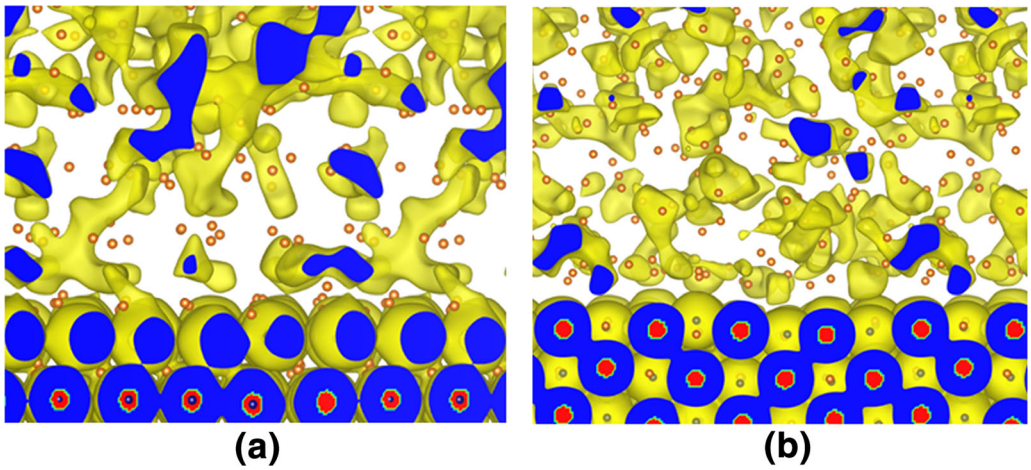

Fig. 9—The iso-surfaces of electron densities at the interfaces between liquid Mg and (*a*) MgO{1 1 1} substrate and (*b*) MgO{0 0 1} substrate. The yellow color responds to the iso-surfaces (ρ_0 = 0.017 e/ Å^3). The blues regions have electron density higher than ρ_0, whereas the red regions are the cross sections around cores of atoms/ions (Color figure online).

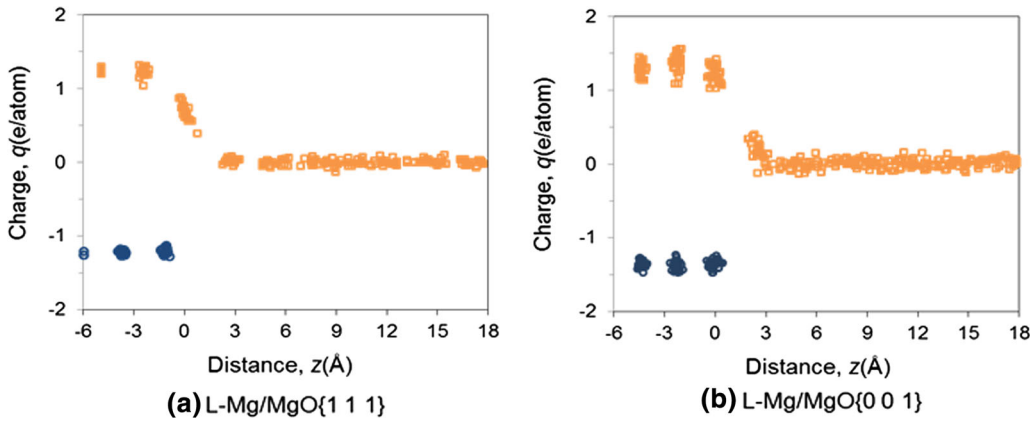

Fig. 10—The charges in the atomic/ionic spheres across the L-Mg/Mg interface with the MgO{1 1 1} substrate and the MgO{0 0 1} substrate. The distance z = 0 corresponds to the center of the substrate surface. The orange squares represent the charges at Mg sites and dark blue spheres at O sites (Color figure online).

adjacent to the flat, non-polar MgO{0 0 1}surface. Therefore, though MgO{0 0 1} is structurally flat, non-polar, and stable at ambient conditions, the chemical interaction between the substrate ions and the liquid Mg atoms induces a rough Mg layer, which is similar to effect of an atomically rough substrate surface.

IV. DISCUSSION

A. *Nucleation Potency of MgO in Liquid Mg*

In heterogeneous nucleation theory, nucleation potency represents the intrinsic capability of a substrate to nucleate a solid phase from the melt.[6] The nucleation potency of a substrate can be quantified by the degree of prenucleation that represents the capability of a substrate for templating atomic ordering in the liquid adjacent to the substrate. Prenucleation can be further quantified by atomic layering normal to the substrate/liquid interface and in-plane atomic ordering parallel to the substrate/liquid interface. The recent studies of prenucleation have identified the following three factors that affect nucleation potency of a substrate[23–26]:

- Structural factor: The lattice misfit between a smooth substrate and a solid has a strong influence on the atomic in-plane ordering but weak on the atomic layering. A substrate surface of a smaller lattice misfit provides better structural templating for heterogeneous nucleation.[23,24]
- Chemical effect: Chemical interaction between the substrate and the liquid also influences structural templating for heterogeneous nucleation. In general, a chemically affinitive substrate promotes prenucleation, whereas a chemical repulsive substrate has lower potency for heterogeneous nucleation.[25]
- Surface roughness: The recent classic molecular dynamics simulation[26] showed that atomically rough surface impedes strongly prenucleation by reducing both atomic layering and in-plane atomic ordering in the liquid adjacent to the substrate.

In light of such understanding of prenucleation, we analyze the nucleation potency of MgO in the L-Mg/MgO system. The previous study[12,16] showed that MgO{1 1 1} has 8.2 pct lattice misfit with solid Mg, suggesting that MgO{1 1 1} is a poor substrate for prenucleation. The present study has shown that regardless the nature of starting surface termination, MgO{1 1 1} in liquid Mg always has a Mg layer as its new terminating surface that contain significant amount of vacancies (Figure 2), rendering MgO{1 1 1} atomically rough. Atomic roughness of a surface can be quantified by the arithmetical mean deviation (R_a):

$$R_a = \left(\sum |\Delta z(j)/d_0|\right) N_z \times 100\,\text{pct} \qquad [3]$$

where $\Delta z(i)$ is the deviation of the ith atom from the atomic plane along the direction perpendicular to the substrate surface, d_0 is the interlayer spacing of Mg{0 0 0 1}, and N_z is the total number of atoms in the layer. When an atom is located in a crystal plane, $\Delta z(i)/d_0 = 0$, when a lattice site is unoccupied (equivalent to an atom is located in the next plane), $\Delta z(i)/d_0 = 1.0$. Our calculation shows that there are 8.0 pct vacancies at the terminating Mg layer of the MgO{1 1 1} substrate (Figure 2). This corresponds to $R_a = 8.0$ pct. Therefore, the large lattice misfit and the large surface roughness make the MgO{1 1 1} extremely poor for structural templating, which in turn results in the poor atomic layering (Figure 3) and in-plane atomic ordering (Figure 8).

The formation of vacancies in the terminating Mg layer in the L-Mg/MgO{1 1 1} system needs further discussion. On one hand, the vacancies at the terminating Mg layer can be at least partially attributed to the charge balance between the atoms in the terminating Mg layer and the liquid Mg adjacent to it. Previous studies in the literature suggested that the polar MgO{1 1 1} surface can be stabilized at ambient conditions with only half of the surface Mg sites being occupied.[14,15] The present study revealed that the terminating Mg ions at the MgO{1 1 1} substrate surface are less charged (about + 0.6 e/Mg on average) as compared with those in the bulk substrate (+ 1.3 e/Mg) (Figure 10). On the other hand, the misfit between the MgO{1 1 1} and α-Mg is large (8.2 pct). Therefore, the formation of vacancies in the terminating Mg layer can be treated as a mechanism to accommodate lattice misfit. In this sense, the 8.2 pct lattice misfit and the 8 pct vacancies in the L-Mg/MgO system may not cause any surprise. However, the relative contributions from accommodation of lattice misfit (structural effect) and charge transfer (chemical effect) warrants further investigations.

In addition, the L-Mg/MgO{0 0 1} system represents another interesting case for heterogeneous nucleation. Structurally, the MgO{0 0 1} substrate also has a large lattice misfit with α-Mg,[12,16] hindering it for heterogeneous nucleation. Chemically, MgO{0 0 1} surface is non-polar under ambient conditions. However, the situation is rather different when MgO{0 0 1} substrate is in contact with liquid Mg. The present study has revealed that the chemical interaction between the MgO{0 0 1} substrate and the liquid Mg results in the formation of a rough 1st layer of Mg atoms in the liquid (Figure 6), which significantly reduces the potency for structural templating of further liquid layers (Figures 4, 5, 7 and 8). As a structurally flat substrate, one would expect pronounced layering since atomic layer is independent of lattice misfits.[23,24] Chemistry analysis showed the chemical interaction exists between the substrate surface and liquid Mg. The liquid Mg atoms adjacent to the oxygen ions are positioned closer to the substrate due to the attractive interaction between oxygen ions in the substrate surface and the Mg atoms in the liquid Mg; whereas liquid Mg atoms adjacent to the Mg ions are positioned further away from the substrate surface because of the repulsive interaction between the Mg ions (Figure 6). Consequently, the 1st layer of liquid Mg atoms becomes rough and less effective for templating atomic ordering in the further layers. Therefore, it can be concluded that the structurally flat MgO{0 0 1} substrate is also impotent for nucleation of solid Mg.

B. *Implications to Grain Refinement of Mg-Alloys*

The *ab initio* molecular dynamics simulations demonstrated that both MgO{1 1 1} and MgO{0 0 1} substrate surfaces are atomically or chemically rough and important for heterogeneous nucleation. However, they may be used for effective grain refinement when no other more potent particles exist in the liquid. In spite of the fact that heterogeneous nucleation as an atomic level activity may occur on all available nucleant particles at a given nucleation undercooling,[12] not all the nucleus can lead to formation of grains in the solidified microstructure. This means that effectiveness of grain refinement depends on the interplay between heterogeneous nucleation governed by the epitaxial nucleation undercooling[11] and grain initiation governed by the free growth criterion.[40] When nucleation undercooling is smaller than the free growth undercooling, grain initiation will be progressive, starting with the largest particle(s) and followed by the progressively smaller ones. Meanwhile, when nucleation undercooling is larger than the free growth undercooling required by many nucleant particles, a large number of nucleant particles can initiate grains at the same time immediately after nucleation, resulting in potentially much more significant grain refinement. The former is called progressive grain initiation, and the later explosive grain initiation.[12]

Recent research work[12,16] suggests that MgO{1 1 1} and MgO{0 0 1} exist in Mg-alloy melt with a small particle size, narrow size distribution, and an extremely large number density (10^{17} m^{-3}). HRTEM work[12,16,18,19] has confirmed that both MgO{1 1 1} and MgO{0 0 1} can act as sites for heterogeneous nucleation of α-Mg. More importantly, it is confirmed that appropriately dispersed native MgO particles can lead to micron level grain size by high pressure die casting of commercial purity Mg,[12] confirming that MgO can be very effective for grain refinement of Mg-alloys under appropriate conditions. This means that once fully dispersed the native MgO particles can effectively grain

refine Mg-alloys without the need for any grain refiner addition. The impotency of both MgO{1 1 1} and MgO{0 0 1} particles in Mg-alloy melt from this study sheds new lights on heterogeneous nucleation, grain initiation, and grain refinement of Mg-alloys.

V. CONCLUSIONS

Using a parameter-free *ab initio* molecular dynamics simulation technique, we investigated the atomic configurations and chemistry of MgO{0 0 1} and MgO{1 1 1} surfaces in liquid Mg. We showed that an atomically rough terminating Mg layer forms on the MgO{1 1 1} substrate in liquid Mg. The simulations also revealed that on the structurally flat MgO{0 0 1} substrate induces a rough Mg layer due to chemical interactions between the ions at the substrate surface and liquid Mg, being similar to the atomically rough MgO{1 1 1} substrate. The surface roughness together with the large lattice misfit with solid Mg makes both MgO{1 1 1} and MgO{0 0 1} substrate ineffective for inducing atomic ordering in the liquid adjacent to the liquid/substrate interface. It is therefore concluded that both MgO{1 1 1} and MgO{0 0 1} are impotent for heterogeneous nucleation of α-Mg. The present results shed new light on grain refinement of Mg-alloys. The native MgO particles are widely available in Mg-alloy melts and may be used for effective grain refinement of Mg-alloys through explosive grain initiation without the need of grain refiner addition.

ACKNOWLEDGMENTS

We thank Dr. H. Men (BCAST, Brunel University London) for the beneficent discussions. Financial support from EPSRC (UK) under grant number EP/N007638/1 is gratefully acknowledged.

OPEN ACCESS

REFERENCES

1. A.L. Greer: *J. Chem. Phys*., 2016, vol. 145, art. no. 211704.
2. M.A. Easton: *Solid State Mater. Sci*., 2016, vol. 20, pp. 13–24.
3. M. Esmaily, J.E. Svensson, S. Fajardo, N. Birbilis, G.S. Frankel, S. Virtanen, R. Arrabal, S. Thomas, and L.G. Johansson: *Progress Mater. Sci*., 2017, vol. 89, pp. 92–193.
4. Y.H. Ali, D. Qiu, B. Jiang, F.S. Pan, and M.Z. Zhang: *J. Alloys Compounds*, 2015, vol. 619, pp. 639–51.
5. D.H. StJohn, M. Qian, M.A. Easton, P. Cao, and Z. Hildebrand: *Metall. Mater. Trans. A*, 2005, vol. 36A, pp. 1669–79.
6. M. Qian, D.H. StJohn, and M.T. Frost: *Scripta Mater*., 2002, vol. 46, pp. 649–54.
7. A. Ramirez, M. Qian, B. Davis, T. Wilks, and D.H. StJohn: *Scripta Mater*., 2008, vol. 59, pp. 19–22.
8. M. Sun, M.A. Easton, D.H. StJohn, G.H. Wu, T.B. Abbott, and W.J. Ding: *Adv. Eng. Mater*., 2013, vol. 15, pp. 373–78.
9. B. Nagasivamuni, G. Wang, D.H. StJohn, and M.S. Dargusch: *J. Crystal Growth*, 2019, vol. 512, pp. 20–32.
10. W.C. Yang, L. Lin, J. Zhang, S.X. Ji, and Z. Fan: *Mater. Lett*., 2015, vol. 160, pp. 263–67.
11. Z. Fan: *Metall. Mater. Trans. A*, 2013, vol. 44A, pp. 1409–18.
12. Z. Fan, F. Gao, and B. Jiang: submitted to *Science*, 2018.
13. H. Men, B. Jiang, and Z. Fan: *Acta Mater*., 2010, vol. 58, pp. 6526–34.
14. P.W. Tasker: *Philos. Mag. A*, 1979, vol. 39, pp. 119–36.
15. C.M. Fang, M.A. Van Huis, D. Vanmaekelbergh, and H.W. Zandbergen: *ACS Nano*, 2010, vol. 4, pp. 211–18.
16. G.S. Peng, Y. Wang, and Z. Fan: *Metall. Mater. Trans. A*, 2018, vol. 49A, pp. 2182–92.
17. Z. Fan, Y. Wang, M. Xia, and S. Arumuganathar: *Acta Mater*., 2009, vol. 57, pp. 4891–4901.
18. Y. Wang, Z. Fan, X. Zhou, and G.E. Thompson: *Philos. Mag. Lett*., 2011, vol. 91, pp. 516–29.
19. Y. Wang, G.S. Peng and Z. Fan: *Magnesium Technology* 2017, eds. K.S. Solank, *et al*. The Minerals, Metals & Materials Series, 2017, pp. 99–106.
20. E.T. Dong, P. Shen, L.X. Shi, D. Zhang, and Q.C. Jiang: *J. Mater. Sci*., 2013, vol. 48, pp. 6008–17.
21. W.W. Xu, A.P. Horsfield, D. Wearing, and P.D. Lee: *J. Alloys Compounds*, 2016, vol. 68, pp. 1233–40.
22. H.-Q. Song, M. Zhao, and J.G. Li: *Modern Phys. Lett. B*, 2016, vol. 30, art. no. 165052.
23. H. Men and Z. Fan: *Comp. Mater. Sci*., 2014, vol. 85, pp. 1–7.
24. H. Men and Z. Fan: *Metall. Mater. Trans. A*, 2018, vol. 49A, pp. 2766–77.
25. C.M. Fang, H. Men, and Z. Fan: *Metall. Mater. Trans. A*, 2018, vol. 49A, pp. 6231–42.
26. B. Jiang, H. Men, and Z. Fan: *Comp. Mater. Sci*., 2018, vol. 153, pp. 73–81.
27. R.R. Reeber, K. Goessel, and K. Wang: *Eur. J. Mineral*., 1995, vol. 7, pp. 1039–47.
28. J.W. Arblaster: *Selected values of the crystallographic properties of the elements*, ASM International, Materials Park, Ohio, 2018.
29. A. Hashibon, J. Adler, M.W. Finnis, and W.D. Kaplan: *Comput. Mater. Sci*., 2002, vol. 24, pp. 443–52.
30. G. Kresse and J. Hafner: *Phys. Rev. B*, 1994, vol. 49, pp. 14251–69.
31. G. Kresse and J. Furthmüller: *Comput. Mater. Sci*., 1996, vol. 6, pp. 15–50.
32. P.E. Blöchl: *Phys. Rev. B*, 1994, vol. 50, pp. 17953–79.
33. G. Kresse and J. Joubert: *Phys. Rev. B*, 1999, vol. 59, pp. 1758–75.
34. J.P. Perdew, K. Burke, and M. Ernzerhof: *Phys. Rev. Lett*., 1996, vol. 77, pp. 3865–68.
35. H.J. Monkhorst and J.D. Pack: *Phys. Rev. B*, 1976, vol. 13, pp. 5188–92.
36. G.A. de Wijs and G. Kresse: *Phys. Rev. B*, 1998, vol. 57, pp. 8223–34.
37. C.M. Fang, R.S. Koster, W.-F. Li, and M.A. van Huis: *RSC Adv*., 2014, vol. 4, pp. 7885–99.
38. R.F.W. Bader: *J. Phys. Chem. A*, 1998, vol. 102, pp. 7314–23.
39. W. Tang, E. Sanville, and G. Henkelman: *J. Phys*., 2009, vol. 21, art. no. 084204.
40. A.L. Greer, A.M. Bunn, A. Tronche, P.V. Evans, and D.J. Bristow: *Acta Mater*., 2000, vol. 48, pp. 2823–35.